GEOMETRIC APPROACH TO DETECT AND REJECT DISTURBANCES APPLIED TO AN ACTIVE SUSPENSION SYSTEM

Bruno de Souza Borges*, Renan L. Pereira*, Fernando H. D. Guaracy*, Fadul F. Rodor*

* *Universidade Federal de Itajubá - Campus Itabira*
Street Irmã Ivone Drumond, 200 - Distrito Industrial II - 35903-087
Itabira, Minas Gerais, Brasil

E-mails: bborges93@hotmail.com, renan.lima@unifei.edu.br, fernandoh@unifei.edu.br, fadulrodor@unifei.edu.br

Abstract— This work investigates a control strategy based on the combination of poles assignment and geometric approach to detect and reject disturbances in an active suspension system. The design procedure has two steps. The first step consists in determining the invariant subspaces for the system according to linear algebra concepts, and use such descriptions to design a full order state observer, which will aid the disturbance detection. The second step is designing a state feedback controller together with a static gain in order to reject the disturbance. After designing the state observer and state feedback controller, some experiments were performed on the active suspension system manufactured by Quanser® Consulting. The experiments resulted in a useful disturbance detection and rejection strategy for implementing in systems where the disturbances are unknown and their rejection is desired.

Keywords— Disturbance detection and rejection, geometric approach, active suspension system.

Resumo— Este trabalho investiga uma estratégia de controle baseada na combinação de alocação de polos e abordagem geométrica para detecção e rejeição de distúrbios em um sistema de suspensão ativa. O procedimento de projeto possui dois passos. O primeiro consiste em determinar os subespaços invariantes do sistema, de acordo com os conceitos de algebra linear, e usar esses subespaços para projetar um observador de estados de ordem completa, o qual auxiliará na detecção da entrada de distúrbio. O segundo passo visa projetar um regulador de estados combinado com um ganho estático para rejeitar os distúrbios. Depois de projetar o observador de estados e o regulador de estados, alguns experimentos foram realizados no sistema de suspensão ativa fabricado pela empresa Quanser®. Por fim, os experimentos resultaram em uma estratégia útil de detecção e rejeição de perturbações para implementação em sistemas onde os distúrbios são desconhecidos e sua rejeição é desejada.

Palavras-chave— Rejeição e detecção de distúrbio, abordagem geométrica, sistema de suspensão ativa.

1 Introduction

Ride quality and comfort are goal attributes in car design. Suspensions have an important role, not only because they help to achieve those, but because they improve the vehicle stability and avoid rollover conditions (Rath et al., 2017). In general, suspensions transfer the force and torque between the wheels and the frame, and attenuate the impact load caused by the pavement and the system vibration.

Passive suspensions are used in most of the conventional cars, and provide disturbance rejection in all frequencies by spring damping systems, but cannot provide attenuation in low and high frequencies. On the other hand, active suspensions are able to dynamically change the damping force according to the sensors measurements and achieve overall better performance. These systems are used in car competitions and some expensive commercial cars (Prattichizzo and Mercorelli, 2000). Moreover, active suspensions aim to absorb the ground and system irregularities and exert null strain on the vehicle body(de Jesús Rubio et al., 2014).

Concerning the application of active suspension systems, different types of control methods for disturbance rejection have been studied. For instance, robust techniques as $\mathcal{H}_\infty$ control, and full-order sliding mode control show good results. However, such approaches do not include any system monitoring that allows the detection of some operation values. In this sense, a strategy based on the combination of a controller to reject the disturbance, with a state estimator to detect the disturbance is suitable. There are some approaches that deal with the disturbance detection and rejection problems (see the paper (de Jesús Rubio et al., 2014) and references therein). Typically, such methods involve complex mathematical manipulations, while a simple pole placement design for observer and state feedback controller may be used.

In this context, the main contribution of this paper consists in the practical investigation of a pole placement strategy based on geometric approach to detect and reject disturbances in an active suspension system. On this approach, the concept of invariance of a subspace for controllability and observability of a linear system is explored. The didactic plant used herein was produced by Quanser® Consulting and has been widely studied in previous articles (da Silva et al., 2013; de Oliveira et al., 2014; Pereira et al., 2017). Its dynamics can be described by a fourth-order system by two masses and two springs, which are independent storage elements that represents a quarter-car model.

This paper is structured as follows: Section 2 presents the concepts of the geometric approach. Section 3 describes the target system of this paper,

its mathematical model and parameters. Section 4 presents the observer and the controller design via geometric approach and the experimental results obtained. Finally, the conclusions are given in Section 5.

1.1 Notation and Definitions

The geometric approach is an alternative theory of control for multivariable linear systems, and uses the concept of subspaces invariance with respect to a linear transformation (Basile and Marro, 1992; Prepaliţă et al., 2012).

Definition 1 *Given a vector space $\mathcal{X}$ over the field of real numbers $\mathbb{R}^n$, a subset $\mathcal{V}$ is subspace of $\mathcal{X}$ if (1) and (2) are true.*

$$\alpha x + \beta y \in \mathcal{V} \quad \forall\ \alpha, \beta \in \mathbb{R}, \quad \forall\ x, y \in \mathcal{V} \tag{1}$$

$$\begin{gathered} A(\alpha x + \beta y) = \alpha A x + \beta A y \\ \forall\ \alpha, \beta \in \mathbb{R}, \quad \forall\ x, y \in \mathcal{X}. \end{gathered} \tag{2}$$

In respect to the transformation $A : \mathcal{X} \to \mathcal{Y}$, let set (3), (4) and (5)

$$\mathrm{Im}(A) := \{y : y = Ax, x \in \mathcal{X}\} \tag{3}$$

$$\ker(A) := \{x : x \in \mathcal{X}, Ax = 0\} \tag{4}$$

$$A^{-1}\mathcal{V} := \{x : v = Ax, v \in \mathcal{V}\} \tag{5}$$

where (3) represents the orthonormalization of A, (4) represents the null space of A, and (5) represents the inverse of a given subspace. The image, the kernel and the invert subspace are subspaces of $\mathcal{X}$ and $\mathcal{Y}$ (Marro, 2007). Moreover, consider $\mathcal{V}$ a n-dimension vector given by (6).

$$\mathcal{V} = \mathrm{gen}\,[v_1, v_2, ..., v_n] \tag{6}$$

where $v_1, v_2, ..., v_n$ are a set of vectors that yield the subspace $\mathcal{V}$ (de Jesús Rubio et al., 2014).

Definition 2 *Considering the transformation $A : \mathcal{X} \to \mathcal{X}$, A is called A-invariant if and only if there is a subspace $\mathcal{V} \subseteq \mathcal{X}$ where (7) can be verified.*

$$A\mathcal{V} \subseteq \mathcal{V} \tag{7}$$

In other words, a system is called A-invariant, if and only if there exists a vector space X such as

$$AV = AX \tag{8}$$

where, given v_i $(i = 1, 2, ..., r)$ as the columns of V, each transformed column is a linear combination of all columns, and if exists vectors x_i that yield $Av_i = Vx_i$ $(i = 1, 2, ..., r)$. Thus, (8) expresses (7) in a compact form. In order to call A-invariant, all the vectors of $A\mathcal{V}$ must be linear combinations of the vectors of $\mathcal{V}$ (Basile and Marro, 1992).

2 Preliminaries and Problem Statement

Consider the system,

$$H := \begin{cases} \dot{x} = Ax + Bu \\ y = Cx + Du \end{cases} \tag{9}$$

where $x \in \mathbb{R}^n$ is the state vector, $u \in \mathbb{R}^m$ is the control input, $y \in \mathbb{R}^p$ is the the system output and $A \in \mathbb{R}^{n\times n}$, $B \in \mathbb{R}^{n\times m}$, $C \in \mathbb{R}^{p\times n}$ and $D \in \mathbb{R}^{p\times m}$ are the state-space matrices. The corresponding linear transformations of each matrix to the subspaces of the system are as follows: $A : \mathcal{X} \to \mathcal{X}$, $B : \mathcal{U} \to \mathcal{X}$, $C : \mathcal{X} \to \mathcal{Y}$ and $D : \mathcal{U} \to \mathcal{Y}$.

The extended system considering the disturbance input is given as,

$$H_d := \begin{cases} \dot{x} = Ax + Bu + Ed \\ y = Cx + Du \end{cases} \tag{10}$$

where d is de disturbance input, and its subspace is given as $E : \mathcal{E} \to \mathcal{X}$.

Moreover, the system (9) can be described as a transfer function,

$$H(s) := C(sI - A)^{-1}B + D \tag{11}$$

where the roots of the polynomial denominator are the poles and the roots of the numerator are the zeros. A system is considered minimum phase, if it does not have any zeros in the right half-plane including the origin. If the system is minimum phase, the transmission zeros are the invariant zeros of the system (Marro and Prattichizzo, 2001).

2.1 Controlled and Conditioned Invariants

Consider the system (9) and let the subspaces $\mathcal{C} = \ker C \subseteq \mathcal{X}$ and $\mathcal{B} = \mathrm{Im}\, B \subseteq \mathcal{X}$.

Theorem 1 *(Marro, 2007) The pair (A,B) is called "Controlled Invariant", if there is a friend space vector F for the output-nulling subspace $\mathcal{V}$ such that (12) is true.*

$$\begin{gathered} (A + BF)\mathcal{V} \subseteq \mathcal{V} \\ \mathcal{V} \subseteq \ker\,(C + DF) \end{gathered} \tag{12}$$

where $\mathcal{V}$ can be calculated from (13).

$$\begin{aligned} &\mathcal{V}_1 = \mathcal{C} \\ &\mathcal{V}_i = \mathcal{C} \cap A^{-1}(\mathcal{V}_{i-1} + \mathcal{B}) \quad (i = 2, 3, 4, ...) \end{aligned} \tag{13}$$

The equation (13) is calculated until convergence. The result is called maximum controlled invariant (Marro and Prattichizzo, 2001) and is denoted as $\mathcal{V}^*$.

Theorem 2 *(Marro, 2007) Similarly, the pair (C,A) is called "Conditioned Invariant", if there is a friend space vector L for the input-containing subspace $\mathcal{W}$ such that (14) is verified.*

$$\begin{gathered} (A + LC)\mathcal{W} \subseteq \mathcal{W} \\ \mathcal{W} \supseteq \mathrm{Im}\,(B + LD) \end{gathered} \tag{14}$$

where $\mathcal{W}$ can be calculated from (15).

$$\begin{aligned} \mathcal{W}_1 &= \mathcal{B} \\ \mathcal{W}_i &= \mathcal{B} + A(\mathcal{W}_{i-1} \cap \mathcal{C}) \quad (i = 2, 3, 4, ...) \end{aligned} \tag{15}$$

The equation (15) is calculated until convergence. The result is called minimum conditioned invariant (Marro and Prattichizzo, 2001) and is denoted as $\mathcal{W}^*$.

Finally, consider the unassigned eigenvalues of (13). These are called the "Invariant Zeros" of the system, and can be considered fixed poles of the matrices (12) and (14) (Basile and Marro, 1992).

2.2 Disturbance Decoupling

Consider the system (9) with the disturbance input (10) and let the subspace $\mathcal{E} = \mathrm{Im}\,(E) \subseteq \mathcal{X}$.

$$\begin{aligned} \dot{\widetilde{x}} &= (A + LC)\widetilde{x} + Bu + Ly \\ \widetilde{d} &= y - C\widetilde{x} \end{aligned} \tag{16}$$

To achieve disturbance decoupling via state feedback controller, the system must be controlled and conditioned invariant, the invariant zeros must be in the complex left half-plane, and the disturbance signal must be inaccessible (Marro, 2007). An option to design a full-order state observer (16) (Figure 1) consists in assigning to gain L the invariant zeros of the system and the remaining poles freely.

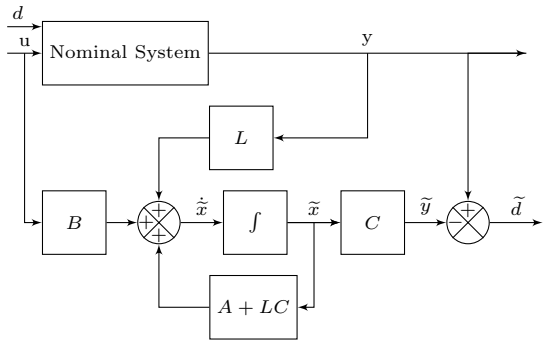

Figure 1: Block diagram of the full-order state observer. Adapted from (de Jesús Rubio et al., 2014)

The disturbance decoupling problem can be achieved if and only if

$$\begin{aligned} \mathcal{E} &\subseteq \mathcal{V}^* + \mathcal{B} \\ \mathcal{E} &\subset \mathcal{V}^* \subset \mathcal{C} \end{aligned} \tag{17}$$

Equation 17 being true, the disturbance is invisible to the state observer (de Jesús Rubio et al., 2014). Similarly, using the detected disturbance $\widetilde{d}$, it is possible to design a state feedback controller through the control law (18)(Figure 2) to reject it, assigning to F the invariant zeros of the system and remaining poles freely. The gain G is a static gain designed arbitrarily, such that generates a null transfer function between y and $\tilde{d}$.

$$u = -F\widetilde{x} + G\widetilde{d} \tag{18}$$

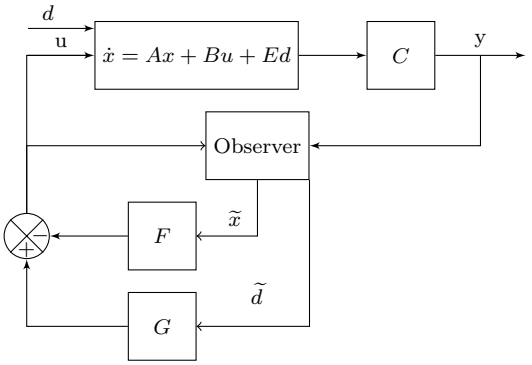

Figure 2: Block diagram of the state feedback. Adapted from (de Jesús Rubio et al., 2014)

3 Description of the Active Suspension System

The active suspension system used here was produced by Quanser® Consulting (Figure 3) and its dynamics can be described as a proper system. The rotary movement of the motor CC1 is converted to linear, which simulates the axial variations of the road. The lower platform represents the road. The middle platform is an unsprung mass representing the wheel and tire. The upper platform is a sprung mass representing the vehicle body. The electric motor CC2 is the active suspension actuator and keeps the upper platform suspended. In addition, the system has two encoders to indicate in a joint way the positions of the three platforms and both have 4096 ticks per revolution (Apkarian and Abdossalami, 2013).

Consider the system (9) and the extended system (10), the linear model provided by Quanser® (Apkarian and Abdossalami, 2013) can be described using state-space representation matrices:

$$\begin{aligned} A &= \begin{bmatrix} 0 & 1 & 0 & -1 \\ -\frac{K_s}{M_s} & -\frac{B_s}{M_s} & 0 & \frac{B_s}{M_s} \\ 0 & 0 & 0 & 1 \\ \frac{K_s}{M_{us}} & \frac{B_s}{M_{us}} & -\frac{K_{us}}{M_{us}} & -\frac{B_s+B_{us}}{M_s} \end{bmatrix}, \\ B &= \begin{bmatrix} 0 \\ \frac{1}{M_s} \\ 0 \\ -\frac{1}{M_{us}} \end{bmatrix}, \; C = \begin{bmatrix} 1 & 0 & 0 & 0 \\ -\frac{K_s}{M_s} & -\frac{B_s}{M_s} & 0 & \frac{B_s}{M_s} \end{bmatrix}, \\ D &= \begin{bmatrix} 0 \\ \frac{1}{M_s} \end{bmatrix}, \qquad E^T = \begin{bmatrix} 0 & 0 & -1 & \frac{B_{us}}{M_{us}} \end{bmatrix} \end{aligned} \tag{19}$$

where the state x_1 is the suspension deflection $Z_s - Z_{us}$, the state x_2 is the vehicle body vertical velocity $\dot{Z}_s$, the state x_3 is the tire deflection $Z_{us} - Z_r$, and the state x_4 is the tire vertical velocity $\dot{Z}_{us}$. The disturbance d is given by the derivative of the road displacement $\dot{Z}_r$ (de Oliveira et al., 2014). The physical interpretation of the parameters as well as their numerical values are given in the Table 1.

Table 1: Active Suspension Parameters

(Apkarian and Abdossalami, 2013)

Parameters		
Symbol	**Name**	**Value**
M_s	Sprung Mass	2.45 Kg
M_{us}	Unsprung Mass	1.0 Kg
Z_s	Load	-
Z_{us}	Wheel and tire	-
Z_r	Road	-
K_s	Suspension Stiffness	900 N/m
K_{us}	Tire Stiffness	2500 N/m
B_s	Suspension Inherent Damping Coefficient	7.5 Nsec/m
B_{us}	Tire Inherent Damping Coefficient	5 Nsec/m

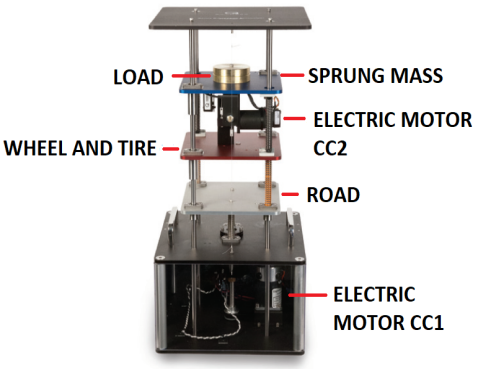

Figure 3: Quanser active supension system. Adapted from (Apkarian and Abdossalami, 2013).

Figure 4 shows the frequency response of the system (10) considering the state-space matrices (19). It is possible to notice that the system has two peaks of amplification, at around 14 [rad/s] and 50 [rad/s]. These points are the critical open loop performance points, which will be better exploited at the Section 4.3.

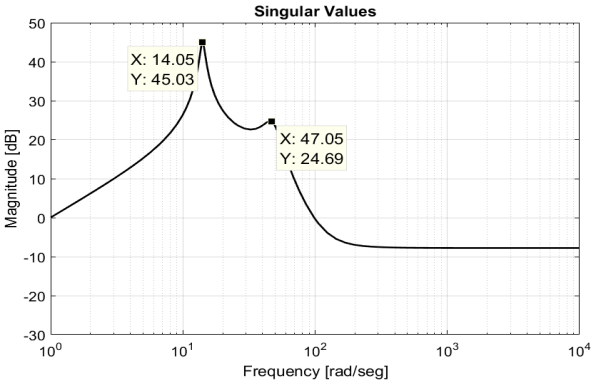

Figure 4: Singular values of the system with the disturbance model.

4 Design and Experimental Results

4.1 State Observer and State Feedback Controller Design

Consider the Single-Input-Multiple-Output system (SIMO) composed by the matrices A, B, C and D described in (19). Since the model describes a Linear Time Invariant system and it is minimum phase, the invariant zeros of (19) are equal to its transmission zeros (11) (Marro and Prattichizzo, 2001).

Moreover, the nominal active suspension system has no zeros, therefore, no fixed poles. Those can be freely assigned. Hence the geometric approach yields (20).

$$P\{A,B,C,D\} = \begin{bmatrix} -6.9453 + 58.7246i \\ -6.9453 - 58.7246i \\ -0.8353 + 16.1843i \\ -0.8353 - 16.1843i \end{bmatrix} \qquad (20)$$
$$Z_i\{A,B,C,D\} = Z\{A,B,C,D\} = [\ ]$$

Assigning to state observer the poles $s_{1,2} = -25.1543 \pm 53.91i$, which are around four times faster than the fastest poles of the system, and testing $s_3 = -1160.5$ and $s_4 = -0.7420$, the observer gain L is given by

$$L = \begin{bmatrix} 0.0245 & -2.3824 \\ -0.0595 & -2.3161 \\ -0.0185 & -2.1042 \\ 2.1024 & 102.4963 \end{bmatrix}. \qquad (21)$$

To determine (15) and (13), it is possible to use a geometric approach toolbox for Matlab®, designed by (Basile and Marro, 1992). Using the toolbox to calculate the minimum conditioned invariant conditions, one obtains (22).

$$\mathcal{W}^* = \text{gen}\left\{\begin{bmatrix} 0 \\ 0 \\ 0 \\ 0 \end{bmatrix}\right\},$$
$$\text{Im}\,(B + LD) = \text{gen}\left\{\begin{bmatrix} -0.0283 \\ -0.0131 \\ -0.0210 \\ -0.9994 \end{bmatrix}\right\}. \qquad (22)$$

The result in (23) shows that the solution for (15) is a null-vector. Since the origin must be solution to every transformation of the type $A : \mathcal{X} \to \mathcal{Y}$, the conditioned invariant problem is solved, and L can be called a friend space vector of $\mathcal{W}_i$.

$$(A + LC)\begin{bmatrix} 0 \\ 0 \\ 0 \\ 0 \end{bmatrix} \subseteq \begin{bmatrix} 0 \\ 0 \\ 0 \\ 0 \end{bmatrix} \supseteq \begin{bmatrix} -0.0283 \\ -0.0131 \\ -0.0210 \\ -0.9994 \end{bmatrix} \qquad (23)$$

For the state feedback control design, the farther poles $s_{1,2} = -8.1 \pm 46.77i$ were kept close to the system poles, while the slower poles $s_{3,4} = -5.25 \pm 13.36i$ were chosen to be around 6 times faster the the system

slower poles. Now, using the pole placement strategy, the state feedback controller F is calculated.

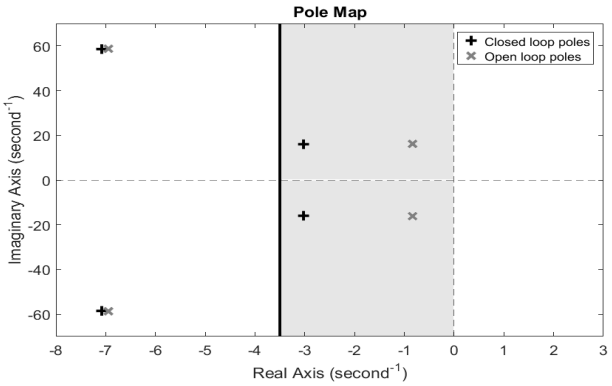

Figure 5: Poles placement.

$$F = \begin{bmatrix} 3.3272 & 15.0114 & -13.6727 & 1.4781 \end{bmatrix}. \quad (24)$$

Using the toolbox to calculate the maximum controlled invariant conditions, one obtains (25).

$$\begin{aligned} \mathcal{V}^* &= \text{gen}\left\{ \begin{bmatrix} 0 \\ 0 \\ 0 \\ 0 \end{bmatrix} \right\}, \\ \ker\left(C + DF\right) &= \text{gen}\left\{ \begin{bmatrix} 0 \\ 0.9088 \\ 0.3488 \\ -0.2291 \end{bmatrix}, \begin{bmatrix} 0 \\ 0 \\ 0.5489 \\ 0.8359 \end{bmatrix} \right\}. \end{aligned} \quad (25)$$

The result in (26) shows that the solution for (13) is a null-vector. For similar reasons of the observer analysis, the controlled invariant problem is solved, and F can be called a friend space vector of $\mathcal{V}_i$.

$$(A + BF) \begin{bmatrix} 0 \\ 0 \\ 0 \\ 0 \end{bmatrix} \subseteq \begin{bmatrix} 0 \\ 0 \\ 0 \\ 0 \end{bmatrix} \subseteq \begin{bmatrix} 0 & 0 \\ 0.9088 & 0 \\ 0.3488 & 0.5489 \\ -0.2291 & 0.8359 \end{bmatrix} \quad (26)$$

Finally, considering the disturbance matrix presented in (19), and using the toolbox to calculate (17), the subspace $\mathcal{E}$ is given by (27).

$$\begin{aligned} \mathcal{E} &= \text{gen}\left\{ \begin{bmatrix} 0 \\ 0 \\ 0.1961 \\ -0.9806 \end{bmatrix} \right\} \\ \mathcal{C} &= \text{gen}\left\{ \begin{bmatrix} 0 \\ 0.7071 \\ 0 \\ 0.7071 \end{bmatrix}, \begin{bmatrix} 0 \\ 0 \\ -1 \\ 0 \end{bmatrix} \right\} = \{c_1, c_2\}. \end{aligned} \quad (27)$$

The image of E satisfies the geometric approach requirements, as shown in (28).

$$\mathcal{E} = -0.1961\ c_1 - \begin{bmatrix} 0 & 0 & 0 & -1.3868 \end{bmatrix}\ c_2 \quad (28)$$

Therefore, from (28), the disturbance is invisible to the observer, and a gain G can be designed to reject the disturbance. Hence, a static gain (29) is then heuristically assigned.

$$G = \begin{bmatrix} 0 - 0.32 \end{bmatrix}. \quad (29)$$

4.2 Simulation Results

In order to evaluate the control strategy, two different road profiles were chosen and simulated in a Matlab® environment.

The first road profile is a step response. It represents a road level variation, and shows its effects on the wheel displacement, and on the body strain. The step has 0.02 [m] of amplitude, length of 6.5 [s] and duty cycle of 50%. The second road profile is a chirp signal proposed by (de Oliveira et al., 2014). The signal has an amplitude 0.0015 [m], and frequency varying linearly from 1 Hz to 10 Hz, during 25 [s]. This signal aims to demonstrate the riding quality. As discussed by (de Oliveira et al., 2014), the critical points seen in Figure 4 represent resonance points, which may cause excessive user discomfort, as well as undesirable body strain and material losses. The necessity of a frequency analysis is also discussed by (Rath et al., 2017) and (Wang et al., 2016).

The open loop response is shown in Figure 6. The tire and the vehicle body have an overshoot of 96.35% and 55.45%, respectively, and virtually no settling time in the given range. Qualitatively, the response has a rather oscillatory behavior throughout the whole simulation, compromising the road handling and the sense of comfort of the rider.

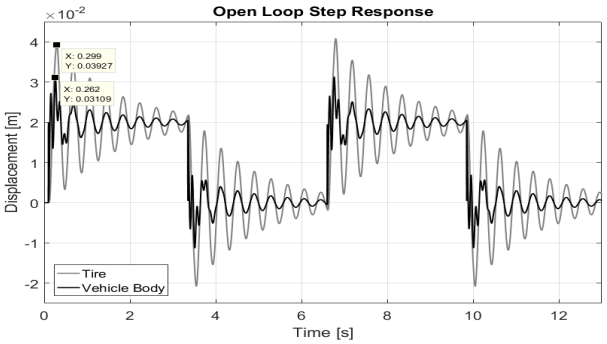

Figure 6: Open loop step response.

In closed-loop (Figure 7), the tire presents an overshoot of 75.05% and settling time of 1.8[s]. The vehicle body shows an overshoot of 44.1%, and a settling time of 1.4 [s]. The displacement of the wheel and the vehicle body reduces 11% and 7%, respectively. The reductions in displacement and the presence of a steady-state ensure a better disturbance damping, and as consequence, diminish suspension travel and enhance riding quality.

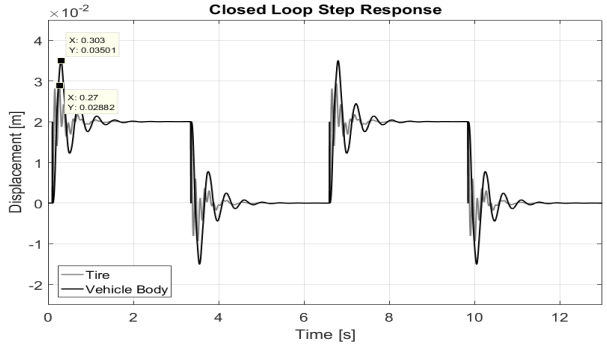

Figure 7: Closed loop step response.

In Figure 8, it can be noted that the disturbance input was successfully detected.

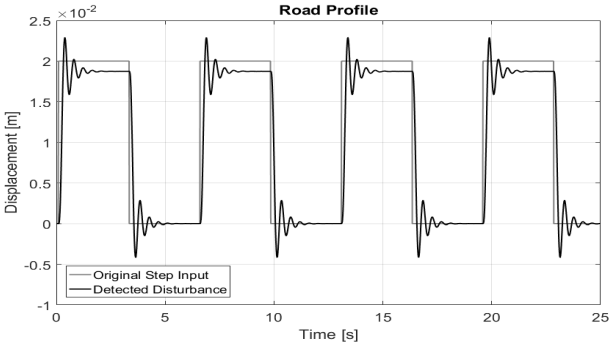

Figure 8: Original and detected step profile.

Using the second road profile, the open loop simulation in Figure 9 shows that the vehicle body suffers an amplification of 8 times the original input around 14 [rads/s]. While the tire not only amplifies the input in the same region, but does it 3 times the original input around 50 [rads/s] as well.

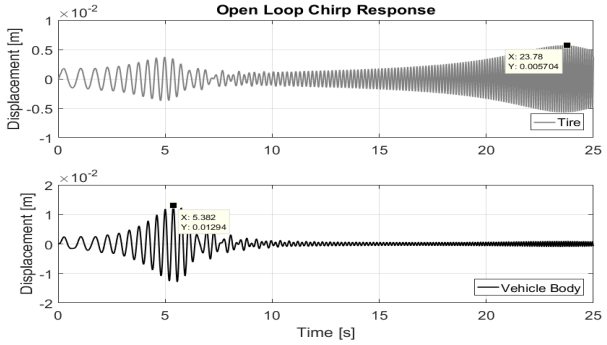

Figure 9: Open loop chirp response.

Evaluating the closed-loop response, an improvement in vehicle body behavior is noticeably observed. However, as seen in Figure 10, the region of 50 [rads/s] has no significant improvement. The reason is that the detected disturbance signal suffers a rather strong attenuation around 50 [rads/s].

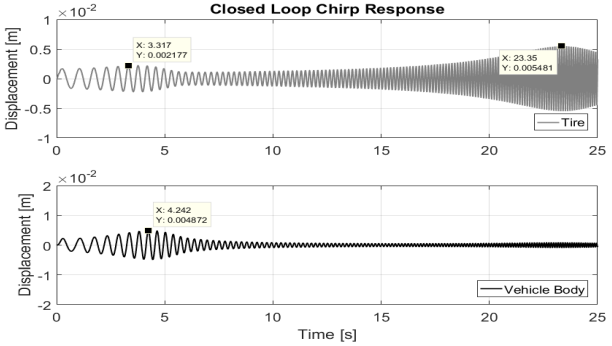

Figure 10: Closed loop chirp response.

4.3 Experimental results

Herein, only the second road profile will be investigated, since many other papers have been using the step response (Apkarian and Abdossalami, 2013; de Jesús Rubio et al., 2014; de Oliveira et al., 2014; da Silva et al., 2013; Pereira et al., 2017). Moreover, the analysis procedure follows the simulation section.

In Figure 11, we can note a slight mismatch with respect to open-loop response (Figure 9). This occurs because the values of stiffness and damping coefficient given in the Table 1 might vary in the experiment.

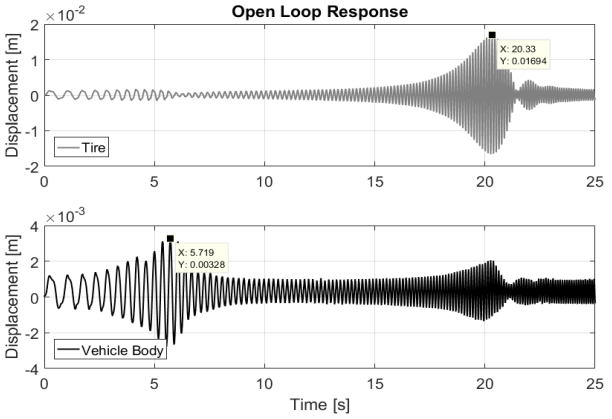

Figure 11: Open-loop response for body and tire displacement.

The disturbance was satisfactorily detected until the most critical region of around 50 [rad/s]. But, since here it is still open loop, the disturbance was not rejected, as shown in Figure 12.

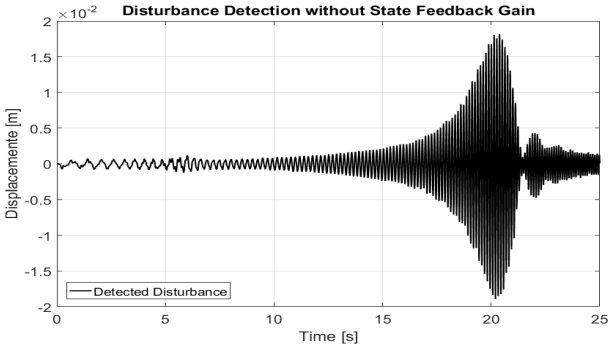

Figure 12: Open-loop response for disturbance detection.

Using the same disturbance signal and from the control law given by (18), (24) and (29), the performance in closed-loop is evaluated. The Figure 13 shows the tire and vehicle body displacements in closed-loop system.

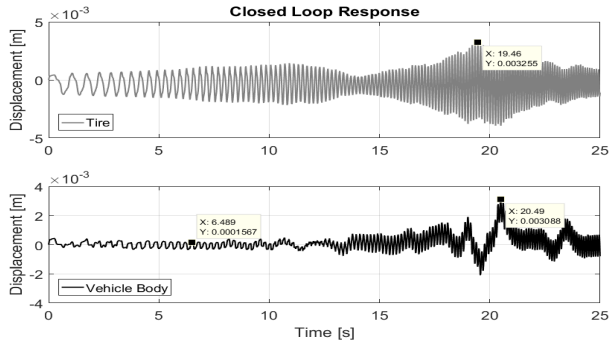

Figure 13: Closed-loop response for body and tire displacement.

The Figure 14 shows the disturbance detected. It is possible to notice that, even though there are some differences between the original signal and the one detected, the closed loop system improved the disturbance detection around 14 [rads/s] and 50 [rads/s]. This represents an overall of 64% detection improvement comparing to Figure 12. Hence, the disturbance detected was successfully rejected.

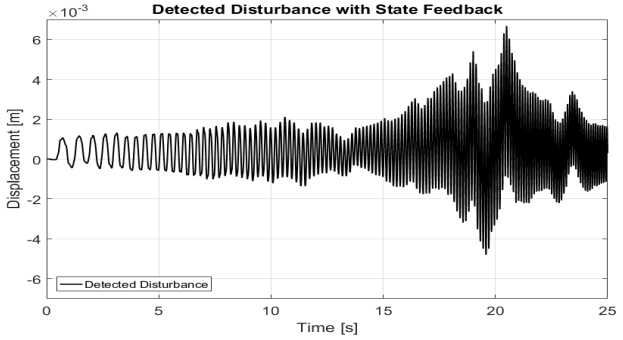

Figure 14: Closed-loop response for disturbance detection.

The active suspension system given by (Apkarian and Abdossalami, 2013) uses the electric motor CC2 to generate the force input (19). In this sense, the Figure 15 shows the current used to generate the required force for the experiment.

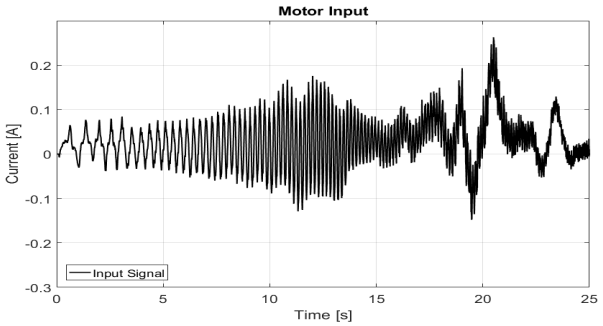

Figure 15: Control effort applied to active suspension system.

5 Conclusions

A practical investigation on the active suspension system using the geometric approach analysis to detect and reject disturbances was presented. To ensure that the disturbance will be rejected is a non-trivial task, but the geometric approach gives good resources to safeguard that. The geometric approach algorithms presents a straightforward theory to be analyzed, once subspaces and linear transformations are trivial calculations, and the maximum and minimum invariant subspaces can be found with computational aid. Once calculated the L and F gains from pole placement strategy, the unknown disturbance observation and decoupling problem has a solution. Finally, the differences between the disturbance injected and the disturbance detected are given not only by some nonlinearity of the system, but by other non-modelled disturbances, such as vibration. Hence, the choice of matrices E and G can also be a future study.

References

Apkarian, J. and Abdossalami, A. (2013). *Laboratory Guide - Active Suspension Experiment for MATLAB®/Simulink® Users*, Quanser Inc.

Basile, G. and Marro, G. (1992). Controlled and conditioned invariants in linear system theory, University of Bologna, Italy.

da Silva, E. R. P., Assunção, E., Teixeira, M. C. M. and Cardim, R. (2013). Robust controller implementation via state-derivative feedback in an active suspension system subjected to fault, *Conference of Control and Fault Tolerant Systems* .

de Jesús Rubio, J., Meléndez, F. and Figueroa, M. (2014). An observer with controller to detect and reject disturbances, *International Journal of Control* **87**: 524–536.

de Oliveira, D. R., Teixeira, M. C. M., Assunção, E., de Souza, W. A., Moreira, M. R. and Silva, J. H. P. (2014). Projeto de controle robusto H_∞ chaveado: Implementação prática em um sistema de suspensão ativa, *XX Congresso Brasileiro de Automática* .

Marro, G. (2007). The geometric approach to control a light presentation of theory and applications, Bologna, Italy.

Marro, G. and Prattichizzo, D. (2001). Linear control theory, University of Bologne and University of Siena, Italy. Summer School on Time Delay Equations and Control Theory, Dobbiaco.

Pereira, R. L., Guaracy, F. H. D., de Paula, C. F. and Pugliese, L. F. (2017). Controle $\mathcal{H}_\infty$ com formatação de malha a tempo discreto aplicado em um sistema de suspensão ativa, *Simpósio Brasileiro de Automação Inteligente* .

Prattichizzo, D. and Mercorelli, P. (2000). On geometric control properties of active suspension systems, *Kybernetica*, Vol. 36, DML-CZ, pp. 549–570.

Prepaliţă, V., Vasilache, T. and Doroftei, M. (2012). Geometric approach to a class of multidimensional hybrid systems, *Balkan Journal of Geometry and Its Applications* **17**: 92–103.

Rath, J. J., Defoort, M., Karimi, H. R. and Chakravarthy, K. (2017). Output feedback active suspension control with higher order terminal sliding mode, *IES* **64**: 1392–1403.

Wang, C., Deng, K., Zhao, W., Zhou, G. and Li, X. (2016). Robust control for active suspension system under steering condition, *Science China Technological Science* **60**: 199–208.